



Since January 2020 Elsevier has created a COVID-19 resource centre with free information in English and Mandarin on the novel coronavirus COVID-19. The COVID-19 resource centre is hosted on Elsevier Connect, the company's public news and information website.

Elsevier hereby grants permission to make all its COVID-19-related research that is available on the COVID-19 resource centre - including this research content - immediately available in PubMed Central and other publicly funded repositories, such as the WHO COVID database with rights for unrestricted research re-use and analyses in any form or by any means with acknowledgement of the original source. These permissions are granted for free by Elsevier for as long as the COVID-19 resource centre remains active.



# Dibenzo-18-crown-6-based carbon paste sensors for the nanomolar potentiometric determination of daclatasvir dihydrochloride: An anti-HCV drug and a potential candidate for treatment of SARS-CoV-2

Yomna M. Ahmed<sup>a</sup>, Sayed S. Badawy<sup>a</sup>, Fatehy M. Abdel-Haleem<sup>a,b,\*</sup>

<sup>a</sup> Chemistry Department, Faculty of Science, Cairo University, Giza, Egypt

<sup>b</sup> Center for Hazards Mitigation, Environmental Studies and Research (CHMESR), Cairo University, Giza, Egypt

## ARTICLE INFO

### Keywords:

Daclatasvir  
Anti-HCV  
SARS-CoV-2  
Carbon paste electrodes  
Dibenzo-18-crown-6  
Potentiometry

## ABSTRACT

Daclatasvir dihydrochloride (DAC) is an anti-hepatitis C virus (HCV) drug that has recently proven to be a promising candidate for the treatment of SARS-CoV-2. Still, there is a lack of sensitive potentiometric methods for its determination. In this work, carbon paste sensors based on dibenzo-18-crown-6 (DB18C6) were fabricated and optimized for the sensitive and selective potentiometric determination of DAC in Daclavicyr® tablets, serum, and urine samples. The best performance was obtained by two sensors referred to as sensor I and sensor II. Both sensors exhibited a wide linear response range of  $5 \times 10^{-9}$  –  $1 \times 10^{-3}$  mol/L, and Nernstian slopes of  $29.8 \pm 1.18$  and  $29.5 \pm 1.00$  mV/decade, with limits of detection,  $4.8 \times 10^{-9}$  and  $3.2 \times 10^{-9}$  mol/L, for the sensors I and II, respectively. Sensors I and II displayed fast response times of 5–8 and 5–6 s, respectively, with great reversibility and no memory effect. Moreover, the sensors exhibited a lifetime of 16 days. For the study of sensors morphology and elucidation of the interaction mechanism, the scanning electron microscope (SEM), Fourier-transform infrared spectroscopy (FTIR), and nuclear magnetic resonance (<sup>1</sup>H NMR) techniques were performed. A selectivity study was performed, and the proposed sensors exhibited good discrimination between DAC and potentially coexisting interferents with sensor II displaying better selectivity. Finally, sensor II was successfully applied for the determination of DAC in the above-mentioned samples, with recovery values ranging from 99.25 to 101.42%, and relative standard deviation (RSD) values ranging from 0.79 to 1.53% which reflected the high accuracy and precision.

## 1. Introduction

Hepatitis C virus infection is a worldwide health problem where its seroprevalence was estimated to be 1% of the world's population [1]. HCV is a major cause of acute and chronic liver disease such as chronic hepatitis, cirrhosis, fibrosis, and hepatocellular carcinoma [2]. HCV infection is endemic in Egypt with a seroprevalence of 40% in some areas making it the highest prevalence rate in the world [3]. For this reason, Egypt developed a national strategy to control and treat HCV infection which aligns with WHO's "global health sector strategy on viral hepatitis", using highly effective regimens of direct-acting antiviral (DAA) therapy such as daclatasvir dihydrochloride, Scheme 1 [4].

Daclatasvir dihydrochloride inhibits HCV replication by binding to the N-terminus of NS5A [5,6], and HCV NS5B RNA polymerase which might resemble RdRp of SARS-CoV-2 [7]. Surprisingly, recent docking

and clinical studies showed that DAC, in addition to another DAA called sofosbuvir, has remarkable binding interactions with SARS-CoV-2 enzymes, and reduces the mortality rates, improves clinical symptoms, and increases the chance of patients' recovery [6–8]. According to Carolina et. al., DAC inhibits the polymerase reaction catalyzed by the SARS-CoV-2 RdRp complex, and inhibits the production of infectious SARS-CoV-2 titers across different cell types, including pneumocytes [9]. The inhibition of the infectious SARS-CoV-2 production in different cells by DAC, is especially significant during the initial stages of the disease and before the invasion of the virus into the parenchymal cells of the lung [6]. That's why there is an urgent need for simple, fast, sensitive, and accurate method for determination of DAC in bulk, pharmaceutical formulations, serum, and urine.

Several methods have been adopted for determination of DAC including, voltammetric [10], which has very narrow working

\* Corresponding author at: Chemistry Department, Faculty of Science, Cairo University, Giza, Egypt.

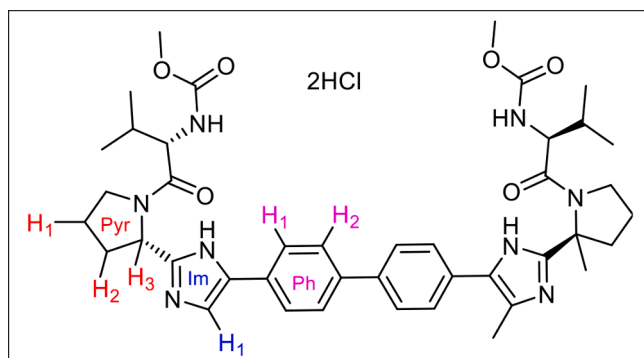
E-mail address: [fatehy@sci.cu.edu.eg](mailto:fatehy@sci.cu.edu.eg) (F.M. Abdel-Haleem).

<https://doi.org/10.1016/j.microc.2022.107276>

Received 2 December 2021; Received in revised form 13 January 2022; Accepted 7 February 2022

Available online 10 February 2022

0026-265X/© 2022 Elsevier B.V. All rights reserved.

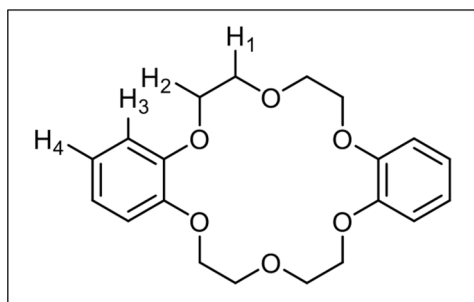


**Scheme 1.** Structure of daclatasvir dihydrochloride. Chemical name: methyl N-[(1S)-1-[(2S)-2-[5-[4-[4-[2-[(2S)-1-[(2S)-2-(methoxycarbonylamino)-3-methylbutanoyl]pyrrolidin-2-yl]-1H-imidazol-5-yl]phenyl]phenyl]-1H-imidazol-2-yl]pyrrolidine-1-carbonyl]-2-methyl-propyl]carbamate dihydrochloride. The numbers don't indicate IUPAC nomenclature, but just for assigning the  $^1\text{H}$  NMR peaks. Ph: phenyl, Im: imidazolyl and Pyr: pyrrolidine.

concentration range (7.0 – 65.0 nM), spectral [11], and chromatographic methods [12], which are expensive, require sophisticated instruments, involve complex procedures, several sample manipulation steps, time-consuming, and in many cases are destructive to the sample.

Potentiometry using ion-selective electrodes (ISEs) on the other hand offers more advantages such as low cost, portability of devices, fast response, wide dynamic range, and compatibility with online monitoring [13][62]. To the best of our knowledge, only two potentiometric methods were reported for the determination of DAC [14,15], but neither of them offered nanomolar determination of DAC, nor applied for its determination in serum samples. Thus, there is a need for development of a new potentiometric technique that offers more sensitivity, and applicable in body fluids.

Carbon paste electrodes (CPEs) offer distinctive advantages over the conventional liquid polymeric membrane electrodes such as low ohmic resistance, the ability of surface renewal, and no need for internal reference solution[63]. In addition, carbon paste represents almost the most flexible electrode material for effective modification[17][63] to improve the analytical performance of the sensor. Lipophilic ionophores represent one of the most common modifiers for CPEs, they include an increasing group of agents, both natural, such as valinomycin, and synthetic, such as crown ethers, that are capable of the selective ion binding[18]. In this study, CPEs based on DB18C6 as a neutral carrier, Scheme 2, were synthesized and optimized with regard to their response characteristics according to the IUPAC guidelines[19] and tested for the determination of DAC in pharmaceutical formulation, serum and urine samples, achieving Nernstian response, reliable Nano-molar determination of the drug, and fast response.



**Scheme 2.** Structure of dibenzo-18-crown-6. The numbering doesn't indicate IUPAC nomenclature, but just for assigning the  $^1\text{H}$  NMR peaks.

## 2. Experimental

### 2.1. Materials

Pure analytical grade DAC, sofosbuvir (SOF), and ledipasvir (LED) were kindly provided by European Egyptian Pharmaceutical Industries (EETI), Alexandria, Egypt. The pharmaceutical formulation Daclavir-ocryl® (60 mg/Tablet) was purchased from a local drug store. Graphite powder (ACROS organics, New Jersey, USA), dioctyl phthalate (DOP, 97.0% Sigma-Aldrich), tricresyl phosphate (TCP, 98.0% Sigma-Aldrich), DB18C6, 98.0% Sigma-Aldrich, sodium tetraphenylborate (Na-TImB, 97% Aldrich chemical company), sodium tertakis(1-imidazolyl)borate (Na-TPB, 99% Alfa Aesar) and tridodecylmethylammonium chloride (TDMAC, 98% Sigma-Aldrich) were used in the construction of the sensors.

Orthophosphoric acid (85 wt%  $\text{H}_3\text{PO}_4$ , Sigma-Aldrich), glacial acetic acid ( $\text{CH}_3\text{CO}_2\text{H}$ , Sigma-Aldrich), and boric acid ( $\text{H}_3\text{BO}_3$ , ACS grade, MISR-Scientific Company) were used in the preparation of Britton-Robinson (B-R) buffer. Copper sulphate pentahydrate (98.5%), chloride salts of sodium (99.8%), potassium (98%), ammonium (99%), magnesium (98%), calcium (97%), manganese (95%) and cobalt (97%) were purchased from ADWIC Cairo, Egypt. Ferric chloride hexahydrate (99%) was purchased from Merck, Germany. D-glucose anhydrous (99%) and starch (ACS grade), were purchased from Fisher Scientific UK. Dopamine hydrochloride (ACS grade), glycine (99%), and DL-leucine (99%) were purchased from Sigma-Aldrich, alanine monohydrochloride (ACS grade) was provided by B.D.H Ltd. London, and DL-histidine monohydrochloride (ACS grade) was purchased from Prolabo, Rue Pelée, Paris.

### 2.2. Apparatus

FTIR (SHIMADZU IR spectrometer), and NMR (Varian Mercury VX-300 NMR spectrometer). Surface images of electrodes were recorded using Quanta FEG 250 scanning electron microscope (FEI Company, Hillsboro, Oregon-USA). Potentiometric and pH measurements were performed using Jenway pH-mVmeter model 3310 (UK), with Ag-AgCl as the reference electrode. High-performance liquid chromatography (HPLC, YL9100 High-performance liquid chromatograph) was used as a reference method for the determination of DAC in commercial tablet samples. Lipophilicity (clogP) was calculated using the ALOGPS 2.1 software[20].

### 2.3. Standard solutions and sample preparation

A stock solution of DAC ( $1.0 \times 10^{-3}$  mol/L) was prepared in Britton-Robinson buffer [21] pH 2.3 and the concentrations ranging from  $1.0 \times 10^{-3}$  mol/L to  $1.0 \times 10^{-9}$  mol/L were prepared by simple serial dilutions using deionized water (18 M $\Omega$ ). For analytical application, five Daclavir-ocryl® tablets were weighed, ground, and an average weight of two tablets were dissolved in a suitable volume and diluted to prepare  $1.0 \times 10^{-6}$  –  $1.0 \times 10^{-5}$  mol/L solutions. For application to body fluids, serum and urine samples were taken from a healthy volunteer (corresponding author) and they were diluted 100 times (taking 0.5 mL serum or urine and complete up to 50 mL) and spiked with a suitable volume of DAC solution to prepare  $1.0 \times 10^{-6}$  –  $1.0 \times 10^{-5}$  mol/L samples. All measurements were performed in a buffered medium. Stock solutions  $1.0 \times 10^{-3}$  M of SOF and LED were prepared; in addition,  $1.0 \times 10^{-1}$  mol/L stock solutions of each of NaCl, KCl,  $\text{NH}_4\text{Cl}$ ,  $\text{CaCl}_2$ ,  $\text{MgCl}_2$ ,  $\text{CuSO}_4$ ,  $\text{CoCl}_2$ ,  $\text{MnCl}_2$ ,  $\text{FeCl}_3$ , dopamine, glycine, alanine, histidine, lysine, glucose, and soluble starch were prepared for the selectivity studies.

### 2.4. CPEs preparation

CPEs were prepared by mixing the dry ingredients in certain weight percent (graphite, DB18C6, and ionic additive) for 10 min in a glass

mortar with a specially made glass pestle, then the plasticizer was added stepwise while mixing. Then the paste was packed well in a piston-driven Teflon holder (resistance was measured to ensure well paste packing, the resistance of optimized sensors in this study was between 9 and 18  $\Omega$ ) [22].

## 2.5. Effect of pH

The influence of the test solution pH on the potential of the prepared electrodes was investigated in two different DAC concentrations, namely,  $1.0 \times 10^{-4}$  and  $1.0 \times 10^{-3}$  mol/L. The pH of the drug solutions was varied using B-R buffer in the range of 2–5, and no further increase in pH was attempted because of the solubility limitation of the drug [23,24]. The potential obtained at each pH value was recorded and plotted against that pH value.

## 2.6. Chemical bonding between DAC and DB18C6 using IR and NMR

FTIR was used for recording the spectra of DB18C6, DAC before and after mixing in dimethyl sulfoxide (DMSO).  $^1\text{H}$  NMR was also used for recording the spectra of DB18C6, DAC before and after mixing the solids in DMSO- $d_6$ , and the chemical shifts ( $\delta$ ) were related to that of the solvent.

## 2.7. Surface characterization of CPEs

SEM and energy dispersive X-ray analysis (EDX) were used for morphological characterization of the optimized sensors. Samples were mounted onto SEM stubs and the applied conditions were a 10.1 mm working distance, with an in-lens detector and an excitation voltage of 20 kV.

## 2.8. Response time, electrode memory, and reversibility

The practical response time of the optimized sensors was measured by successively immersing the electrodes in a series of DAC solutions. In each solution the DAC concentration is increased by a value of half a decade from  $1.0 \times 10^{-9}$  to  $1.0 \times 10^{-3}$  mol/L. Time reading was recorded at the same instance the electrode was introduced into the sample solution.

Electrode memory and reversibility were tested by measuring the potential response of the sensors successively from high-to-low concentrations and vice versa ( $1.0 \times 10^{-4}$  and  $1.0 \times 10^{-3}$  mol/L).

## 2.9. Water layer test

To test the formation of an aqueous layer, the sensors' potential was recorded after successively introducing the electrodes into  $1.0 \times 10^{-3}$  mol/L DAC solution for 30 min,  $1.0 \times 10^{-3}$  mol/L  $\text{Na}^+$  solution for 30 min, and  $1.0 \times 10^{-3}$  mol/L DAC solution for 30 min.

## 2.10. Potentiometric selectivity

Selectivity coefficients were determined using the separate solution method (SSM) and the matched potential method (MPM). In SSM,  $10^{-3}$  mol/L solution was used for both DAC and interfering ions (B), and the selectivity coefficient ( $K_{\text{DAC,B}}^{\text{pot}}$ ) was calculated according to the equation [25]:

$\log K_{\text{DAC,B}}^{\text{pot}} = \frac{(E_B - E_{\text{DAC}})}{S} + (1 - \frac{z_{\text{DAC}}}{z_B}) \log a_{\text{DAC}}$ , where  $E_B$  and  $E_{\text{DAC}}$  are the electrode potentials of  $10^{-3}$  mol/L solution of interfering cations, and DAC, respectively,  $S$  is the slope of the calibration graph, and  $z_{\text{DAC}}$  and  $z_B$  are the charges of DAC and the interfering ion, respectively, and  $a_{\text{DAC}}$  is the activity of DAC solution.

For the application of MPM, the potential of a reference solution containing a fixed level of primary ion ( $a_{\text{DAC}}$ ) is measured, and then a

known activity ( $a_{\text{DAC}}$ ) of the primary ion is added to that reference solution and the potential difference is recorded. In a second experiment, interfering ion with activity ( $a_B$ ) is added to an identical reference solution until the same potential change is reached. The MPM selectivity coefficient is calculated using the equation:

$$K_{\text{DAC,B}}^{\text{pot}} = \frac{a_{\text{DAC}} - a_{\text{DAC}}}{a_B}$$

For larger selectivity [26], the range of measurements by this MPM was extended by using a more dilute reference solution ( $10^{-6}$  mol/L) and a more concentrated foreign species solution in the range of  $10^{-3}$  –  $10^{-1}$  mol/L [27].

## 2.11. Lifetime

The lifetime of the optimized sensors was tested by measuring the performance characteristics of the sensors for 20 days.

## 2.12. Analytical application

The proposed method was used for the determination of DAC in Daclavriocryl® tablets, spiked serum, and urine samples. The analysis was performed using the standard addition method due to its ability to compensate for the effect of the matrix.

In the standard addition method, small increments of DAC standard were added to 25 mL aliquot samples of different concentrations, and the potential difference was recorded for each addition. The concentration of the sample can be calculated by the following equation [28]:

$$C_x = C_s \left( \frac{V_s}{V_x + V_s} \right) \times \left[ 10^{\Delta E/S} - \left( \frac{V_x}{V_x + V_s} \right) \right]^{-1}$$

where  $C_x$  is the concentration to be determined,  $V_x$  is the volume of the sample,  $C_s$  and  $V_s$  are the concentration and volume of the added standard, respectively,  $\Delta E$  is the potential change after adding  $V_s$ , and  $S$  is the slope of the calibration graph.

HPLC method was used as a reference method for the determination of DAC in tablet formulation. Reversed-phase C18 column was used as the stationary phase, phosphate buffer (10 mM, 1 mL triethylamine  $\text{L}^{-1}$ ): acetonitrile (60:40 v/v) was used as the mobile phase with a flow rate of 2 mL/min with UV detection at 312 nm [29].

## 3. Results and Discussion

### 3.1. Effect of electrode composition and modifiers

Performance characteristics of ion-selective electrodes largely depend on the nature and amount of different components of the electrodes; so, several CPEs -containing 1% DB18C6 as a neutral carrier ionophore- were prepared and tested for the determination of DAC.

From the data in Table S1 (in supplementary materials), sensor 1 containing only DB18C6 with no ionic additives exhibited a Sub-Nernstian response towards DAC of 14.8 mV/decade. It is well-established that, neutral carrier-based ISEs are greatly influenced by the presence of ionic sites. These sites facilitate the ion-exchange process at the membrane/solution interface [18][64]. For this reason, 1% TDMAC cationic site was added in sensor 2; but the slope decreased to 10.7 mV/decade indicating that DAC is cationic in the sample solution; and thus it is more suitable to use anionic additive instead. 1% Na-TPB anionic site was introduced to sensor 3, resulting in a Super-Nernstian slope of 48.7 mV/decade. The amount of Na-TPB was reduced to 0.5% in sensor 4 showing more promising results in terms of the Nernstian response (29.8 mV/decade), the wide linear dynamic range ( $5.0 \times 10^{-9}$  –  $1.0 \times 10^{-3}$  mol/L), and the low detection limit ( $4.8 \times 10^{-9}$  mol/L). The great enhancement of the electrode response by Na-TPB is due to the fact that anionic additives offer many advantages to neutral carrier-based

ISEs such as improving the selectivity to the primary ion, reducing paste resistance [30,31], reduction or elimination of interference by co-ions, and minimizing electrode response time[32].

The type of plasticizer is known to influence the electrochemical properties of CPEs, as it dissolves the ionophore and anionic additive and affects the overall mobility of paste ingredients[20][64]. It also influences the dielectric constant ( $\epsilon$ ) of the paste and affects the extraction of analyte species from the sample solution[33][64]. As mentioned earlier, good performance characteristics were obtained with sensor 4 when TCP ( $\epsilon = 6.9$ )[34][64] was used as a plasticizer. However, when the plasticizer was changed to DOP ( $\epsilon = 5.1$ )[34][65] in sensor 5 the slope and upper detection limit diminished to 24.9 mV/decade and  $1.0 \times 10^{-4}$  mol/L, respectively, and the lower detection limit was increased to  $2.8 \times 10^{-8}$  mol/L.

It has been reported that the nature of aromatic groups linked to boron in the anionic site has a great influence on target ion recognition and selectivity[35][66], and thus another borate anionic additive salt (Na-TImB) was used in sensors 6–10. Sensors 6–8 were fabricated using TCP plasticizer, but the performance characteristics of these electrodes were worse than that obtained by sensor 4 (containing Na-TPB), as they have narrower linear dynamic ranges. However, when the plasticizer was changed from TCP to DOP in sensor 9 with 0.25% Na-TImB, it showed Nernstian behavior (29.5 mV/decade) with a wide linear range ( $5.0 \times 10^{-9}$  –  $1.0 \times 10^{-3}$  mol/L) and a low detection limit ( $3.2 \times 10^{-9}$  mol/L). Furthermore, when the percent of Na-TImB was increased to 0.75% in sensor 10, the slope, linear range, and the detection limit diminished to 22.2 mV/decade,  $5.0 \times 10^{-8}$  –  $1.0 \times 10^{-4}$ , and  $2.8 \times 10^{-8}$  mol/L, respectively.

The two optimized sensors -sensors 4 and 9, referred to as sensors I and II, respectively- differ in the anionic site type, and the plasticizer type. Sensor I containing Na-TPB (clogP = 6.89) showed the best performance in the presence of TCP (clogP = 4.87) plasticizer, and on the other hand sensor II containing Na-TImB (clogP = 0.54) did the same but in presence of DOP (clogP = 6.86) plasticizer. In other words, the results imply a synergistic effect between a less lipophilic plasticizer and a more lipophilic anionic additive, and vice versa. This could be explained based on that there is some specific interaction[36] between each (Na-TPB and TCP) and (Na-TImB and DOP), or that both components control the overall membrane lipophilicity, which in turn affects the process of complexation between the ionophore and the target ion.

In terms of the performance characteristics of the fabricated sensors, sensors 4 and 9 showed the best Nernstian slopes, wide linear ranges, and lowest detection limits; therefore, these sensors were chosen for further studies. These sensors will be referred to as sensor I and sensor II, respectively, and their corresponding calibration graphs are shown in

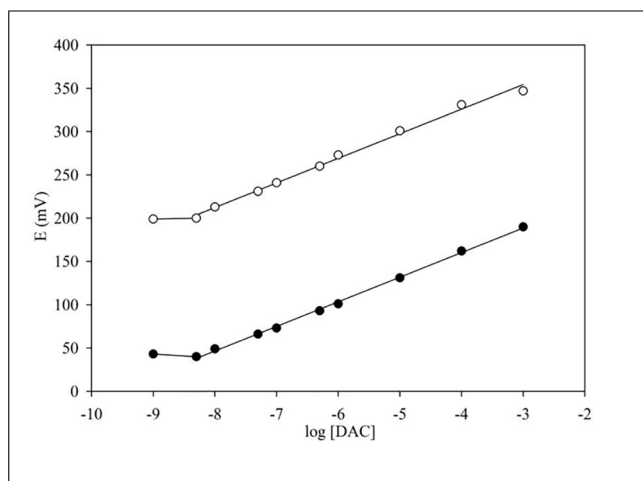


Fig. 1. Calibration graphs of sensors I (●) and II (○).

Fig. 1.

### 3.2. Effect of pH

As shown in Fig. 2, sensors I and II were not sensitive to pH change up to pH 4, after which at pH 4.5 white turbidity was observed in the sample solution, accompanied by a large decrease in electrodes' potential. This turbidity could be due to the precipitation of DAC due to its solubility limitation [23,24], and thus causes a decrease in the concentration of dissolved DAC cations which explains the decrease in the measured potential. The decrease in potential is also confirmed by the pKa values of DAC, 3.82 and 6.09 [37], as after pH 3.82 the ionization state of DAC changes which will, in turn, affect the potential value recorded. Similar behavior was reported by Derar et. al. [14].

### 3.3. Chemical bonding between DAC and DB18C6

Supramolecular chemistry has drawn great attention in the field of ISEs based on molecular recognition. The mechanism of action of supramolecular-based potentiometric sensors depends on host-guest chemistry, where supramolecular assemblies are held together with reversible noncovalent interactions that encompass a wide range of binding energies ranging from electrostatic interactions, H-bonding, hydrophobic, and  $\pi$ - $\pi$  interactions[38].

Recent studies show that DAC exhibits unusual complexation behavior with different forms of supramolecular cyclodextrin hosts, namely  $\gamma$ -cyclodextrin[39] and methylated  $\beta$ -cyclodextrins[40]. Pederson has discovered dibenzo-18-crown-6 in 1967 [41], and since then it has been widely studied for metal complex formation; it was only recently used for drug ion sensors[42]. DB18C6 has a great ability to form inclusion complexes with different species, such as  $\text{Na}^+$ ,  $\text{K}^+$ [43],  $\text{Ca}^{2+}$ [44]; these species will be discussed in the selectivity study. According to the literature, 18-crown-6 has proven to be a good receptor for the protonated N-terminus of an amino acid[45]; such protonated N sites are present in DAC structure, revealing that DB18C6 is a suitable host for the analyte under study. To study the nature of chemical bonding between the ionophore DB18C6 and DAC, FTIR and  $^1\text{H}$  NMR spectra were recorded.

On evaluating Table 1 and Fig. 3, broadening in peak 1 was observed, which indicates the H-bonding interaction between both compounds. Besides, the lowering in N—H stretching vibrational frequency from  $3441.01 \text{ cm}^{-1}$  in free DAC to  $3425.58 \text{ cm}^{-1}$  in the mixture can also indicate NH- $\pi$  interaction[46]. Furthermore, a redshift was observed in peaks 2 and 3 (aromatic C—H peaks) suggesting the presence of CH- $\pi$  and  $\pi$ - $\pi$  interaction[47], although theory predicts a blueshift for such interactions, experimental results presented here reports otherwise, moreover, Lemmens et. al. [47] and Erlekam et. al[48] also documented redshifts.

$^1\text{H}$  NMR spectra, of DB18C6, DAC, and their mixture are shown in Fig. S1 and the corresponding chemical shifts of the peaks are represented in Table S2.  $\pi$ - $\pi$  interaction mentioned earlier is further confirmed by the up-field shifts of NMR peaks assigned for the aromatic protons of the phenyl groups in both molecules and in the two imidazole  $\text{H}_1$  in DAC. In addition, the hydrogens of  $-\text{CH}_2$  moieties in the ring structure of DB18C6 also experienced up-field shifts, which can be explained by the possibility of CH- $\pi$  interactions [49] between these hydrogens in the crown ether and the aromatic phenyl or imidazole in DAC. Similar up-field shifts were observed in pyrrolidine protons H-1,2,3, suggesting CH- $\pi$  interactions between these protons in DAC and the aromatic phenyl groups in DB18C6. In addition, the secondary amide proton in DAC experienced a downfield shift, which can be attributed to H-bonding [50] between NH in DAC and the oxygen atoms in the DB18C6 cavity. DB18C6 can interact at both sides of DAC, or in the middle of the compound, as in Scheme 3.

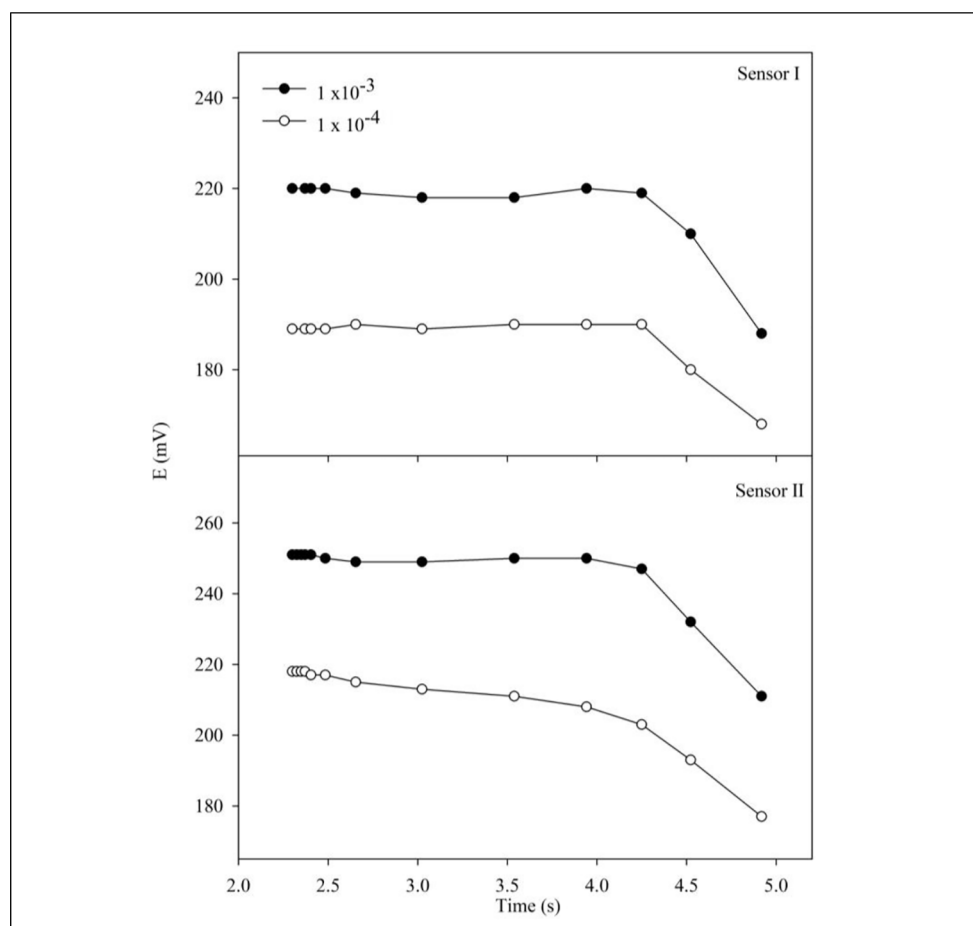


Fig. 2. The effect of pH on the potential response of sensors I and II.

Table 1

FTIR data for DAC and a mixture of DB18C6 and DAC.

DAC ( $\text{cm}^{-1}$ )	DB18C6 + DAC ( $\text{cm}^{-1}$ )	Peak	Observation	Suggested interaction	Ref.
3441.01	3425.58	1	Peak broadening and decrease in wavenumber	H-bonding and NH- $\pi$ interaction	[46]
2993.52	3001.24	2	Increase in wavenumber	CH- $\pi$ and/or $\pi$ - $\pi$ interaction	[47]
2908.65	2916.37	3	Increase in wavenumber	CH- $\pi$ and/or $\pi$ - $\pi$ interaction	[47]

### 3.4. Surface characterization

The signal transduction and thus the response of electrochemical sensors is related to their physicochemical morphology and surface architecture that connects the ionophore with the analyte in sample solution at the nanometer scale[51].

The SEM images of sensors I and II in Tables 2 and 3 show that the pastes exhibit a granular sub microstructure indicating the high surface area of the sensors. On comparing SEM images of the two sensors, it can be observed that sensor II has fewer white spots than sensor I, suggesting higher solubility of electrode components in the plasticizer[52], which may be the reason that sensor II offer lower detection limit than sensor I.

Mapping data in Table 3 show the surface distribution of different elements, C (representing graphite, plasticizer, and DB18C6), O (present in DB18C6), B (belong to the ionic site, Na-TPB or Na-TImB), N in Na-TImB, and P (specific for TCP plasticizer). As can be seen, the different

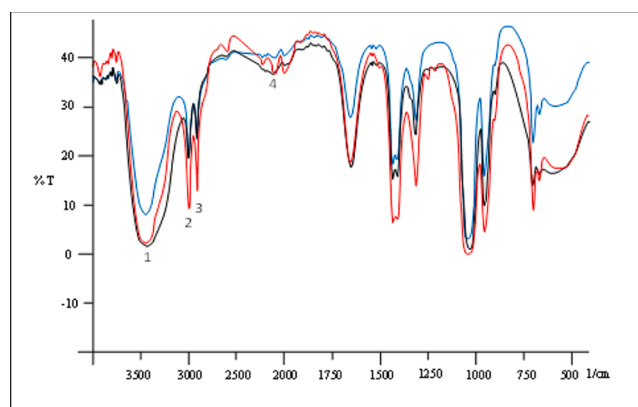
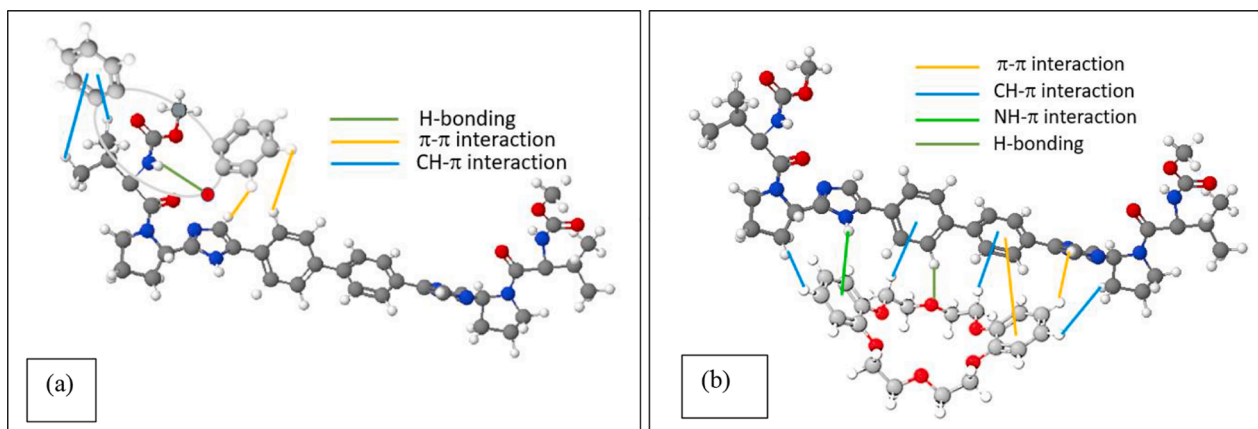


Fig. 3. FTIR spectra of DB18C6 (red), DAC (blue) and DB18C6 + DAC (black).

elements are evenly distributed at the surface of the paste with high homogeneity, indicating the good solubility of the ionophore and exchanger in the plasticizer. EDX and corresponding w% of different elements of sensors I and II are shown in Fig. S2, the appearance of well-defined peaks of elements related to the ionophore and ionic site approves the effective modification of the carbon pastes.

### 3.5. Response time, electrode memory, and reversibility

One of the critical factors in the use of ISEs in routine analysis is the so-called response time. Practical response time has been defined as the



**Scheme 3.** Representation of the complexes formed between DAC and DB18C6. The inclusion complex between the cavity (represented by the oval shape for simplification) of DB18C6 and one of DAC terminals (a), and another possible complexation mode showing the host and guest in parallel positions (b). Dark grey and silver: carbon, white: hydrogen, red: oxygen: blue: nitrogen.

**Table 2**

SEM images of sensor I and sensor II.

SEM images	
Sensor I	Sensor II

time that elapses between the instant at which the ISE and the reference electrode are brought in contact with the sample solution, during which potential (E) changes by 90% of the final value[53]. As presented in Fig. 4 sensor I showed a response time of <5 sec for low concentrations ( $5 \times 10^{-9}$  –  $1 \times 10^{-6}$  mol/L), and about 8 sec for high concentrations ( $1 \times 10^{-5}$  –  $1 \times 10^{-3}$  mol/L), while sensor II showed a response time of about 5 sec for low concentrations, and about 6 sec for high concentrations. The fast response by the sensors may be attributed to the assumption that the additive (Na-TPB or Na-TiMB) lowers the activation barrier for the cation-exchange reaction at the membrane/solution interface and thus reduces the time response after an activity step[54]. In addition, the small electrode resistance plays an important role in shortening time responses[55].

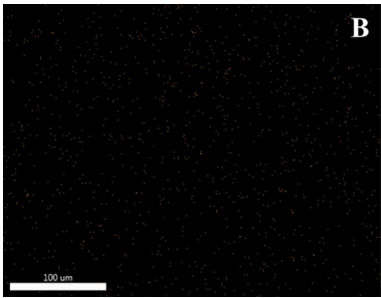
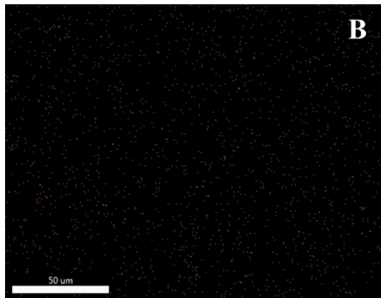
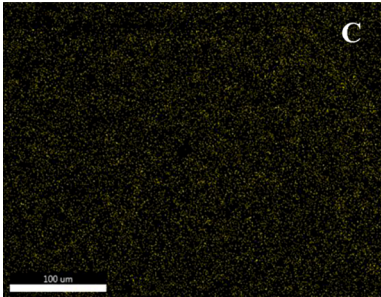
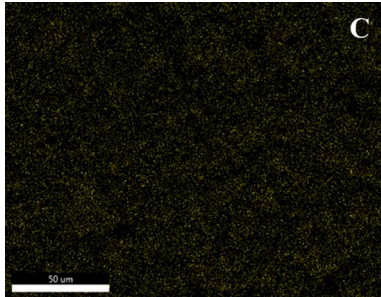
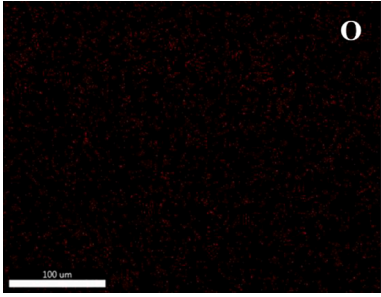
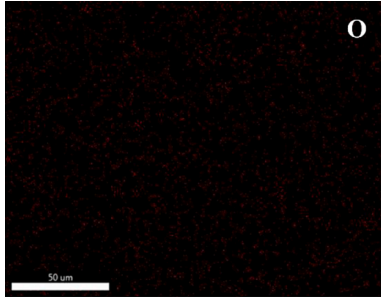
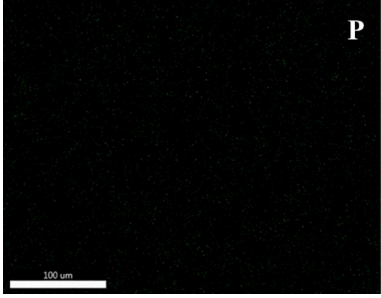
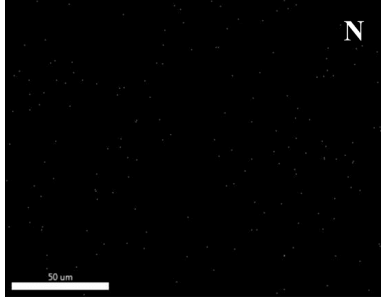
The repeatability of potential reading was tested by immersing each sensor in successive high-to-low concentrations ( $1 \times 10^{-4}$  and  $1 \times 10^{-3}$

mol/L). As shown in Fig. 5, the sensors possess excellent reversibility i. e., have no memory effect, this may be explained by the high reversibility of ionophore-analyte complexation and fast exchange kinetics of association-dissociation interaction at the interface between the electrode surface and the sample solution[56][67].

### 3.6. Water layer test

Early solid contact electrodes had potential drifts and did not exhibit good detection limits which was recently suggested to be due to the poor adhesion between membrane and underlying electron conductor which can lead to the formation of a water layer, acting as a reservoir for electrolyte [57]. The water layer test or the so-called Morf test was introduced by Morf et al. [58] to test the potential stability of solid contact electrodes such as CPES.

**Table 3**  
SEM images with elemental mapping of sensor I and sensor II.

SEM images with elemental mapping	
sensor I	sensor II
	
	
	
	

As shown in Fig. 6, both sensors exhibited stable EMF reading in  $10^{-3}$  M DAC solution for 30 min, after which the solution was changed to  $10^{-3}$  M  $\text{Na}^+$  solution and the sensors also showed a fast response and potential stability, and the decrease in potential proves the selectivity of the sensors towards DAC. Upon changing the solution back to  $10^{-3}$  M DAC the potential is restored with high stability proving the absence of water film reservoirs formed between the carbon paste and stainless-steel rod contact. It turns out that the high hydrophobicity of carbon paste and its tight packing -which is aided by the modern design of piston-driven Teflon holders that yield pastes with good mechanical properties[59]- prevent the formation of a water layer.

### 3.7. Selectivity

The selectivity of sensors I and II was evaluated by calculating  $\log K_{\text{DAC,B}}^{\text{pot}}$ , assessed by the SSM and MPM against several inorganic, organic

species that may coexist with DAC and two of the formulated drugs SOF and LED, since this method will be applied in the determination of DAC in pharmaceutical tablet, serum, and urine samples.

As shown in Table 4 and Fig. S3, it can be noted that all tested species don't significantly interfere with the determination of DAC; this is confirmed as all  $\log K_{\text{DAC,B}}^{\text{pot}}$  values were less than  $-1$ , except for  $\text{K}^+$  in the case of sensor I using SSM, where the value was  $-0.57$ . This behavior is not surprising as many studies proved that the ionophore, DB18C6, has a great selectivity towards  $\text{K}^+$  [43]. However, when the MPM was applied, it gave a better selectivity coefficient value of  $-2.73$  against  $\text{K}^+$ . This large difference may be due to the fact that SSM has many limitations in the case of ions with non-Nernstian responses and that of unequal charges[60].

On the other hand, sensor II showed no interference from  $\text{K}^+$  as it offers a much lower  $\log K_{\text{DAC,K}^+}^{\text{pot}}$  value of  $-2.37$  using SSM and  $-2.98$

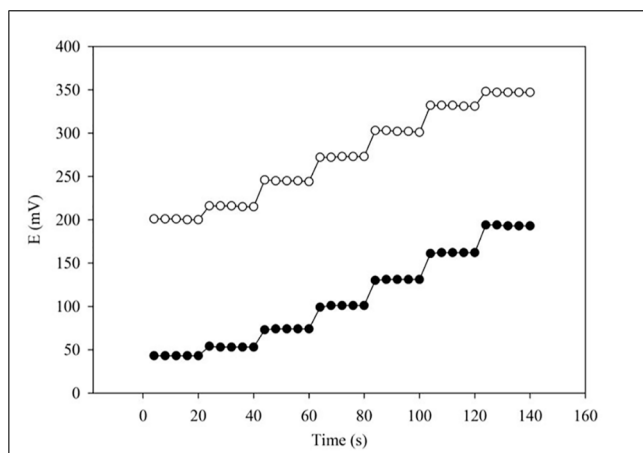


Fig. 4. The dynamic response time of sensors I (●) and II (○).

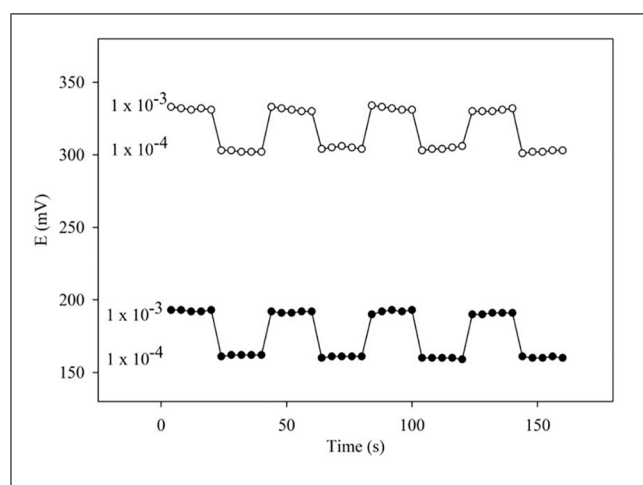


Fig. 5. Electrode memory and reversibility of sensor I (●) and II (○).

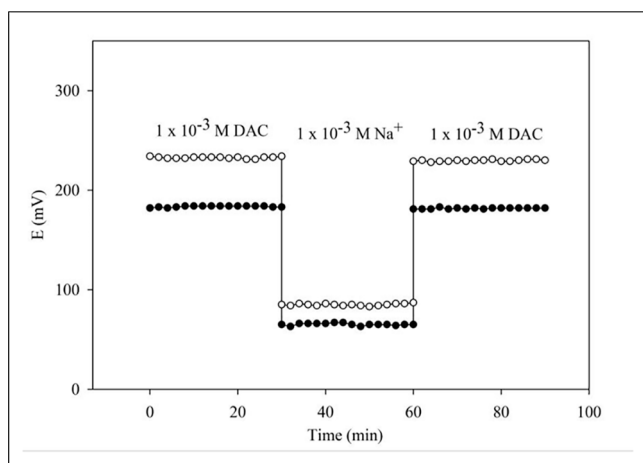


Fig. 6. Water layer test of sensors I (●) and II (○).

using MPM. The presence of Na-TImB in sensor II plays an important role in enhancing the selectivity of the electrode. Alaviuhkola T. et. al. reported that the nature of aromatic unit bound to boron in the ionic sites strongly affects the selectivity of the ISE[36], the boron center in TPB is attached to four phenyl groups, while in TImB it is linked to four

N atoms, this could result in high extraction of DAC from the solution phase due to the higher extent of binding to the imidazole groups in Na-TImB through H-bonding, CH- $\pi$  and/or  $\pi$ - $\pi$  interaction than in case of Na-TPB. In addition, the binding affinity of DB18C6 towards  $K^+$  is affected by the solvent[43], thus, the better selectivity results obtained by sensor II could be related also to the use of DOP plasticizer with low polarity which facilitates the interaction with DAC. In sensor I the more polar TCP has greater interaction with  $K^+$  than the less polar DOP[33].

Since the used ionophore DB18C6 was reported to respond to several cations, sensors I' and II' were made with the same composition as sensors I and II, respectively, only lacking the ionophore, to investigate its effect on the selectivity of the electrodes. The composition (% w/w) of sensor I' is 69.75% graphite, 29.75% TCP, and 0.5% Na-TPB, and that of sensor II' is 69.875% graphite, 29.875% DOP, and 0.25% Na-TImB. On comparing the selectivity coefficient values obtained using sensors with (I and II) DB18C6 and without (I' and II') DB18C6, it can be noticed from Table 4 that DB18C6 has improved the selectivity of the sensors against all tested species, except for  $K^+$ , where the sensors without the ionophore exhibited better selectivity for DAC over  $K^+$ , in other words, the incorporation of DB18C6 in the electrode cocktail increased its response to  $K^+$ . This phenomenon, as mentioned earlier, is due that DB18C6 has the strongest binding affinity towards  $K^+$  among all other alkali metal cations[43].

From the data in Table 4, it is evident that sensor II has generally better selectivity towards DAC than sensor I, and for this reason, sensor II was chosen to be applied for the determination of DAC in pharmaceutical and biological samples.

### 3.8. Lifetime

It is well-established that the primary reason for limited lifetimes of ISEs is caused by the loss of plasticizer, ionophore, and/or the ionic site from the sensor due to leaching of these components into the sample [33]. The lifetime of sensors II was tested by measuring the performance characteristics of the sensor for 20 days. It was found that after 16 days the sensor exhibited good response slope of 25.3 mV/decade, as observed in Table S3. Sensor II showed great sensitivity as it was used for 20 days, and the lower detection limit (LDL) was only increased from  $3.2 \times 10^{-9}$  to  $5.5 \times 10^{-9}$  mol/L, while the upper detection limit (UDL) was reduced from  $1 \times 10^{-3}$  to  $1 \times 10^{-6}$  mol/L, this deviation from linearity at the UDL may be due to Donnan failure[61].

### 3.9. Analytical application

The optimized sensor was successful in determining DAC in pharmaceutical formulation (tablet) and in spiked biological fluids (serum and urine) using standard additions method; the results are summarized in Table 5. All the recovery values were between 99.25 and 101.42% and the RSD values were between 0.79 and 1.53% indicating high precision and accuracy and thus high reliability.

The results obtained from the determination of 5  $\mu$ mol/L DAC in Daclavriocryl® by sensors II were compared to HPLC[29] as a reference method, and the HPLC chromatogram is represented in Fig. S4. Statistical F- and t-tests were applied, and the calculated values, as observed in Table 6, are less than the critical theoretical values, indicating that there is no significant difference between the precisions and means of both methods at 95% confidence limit ( $P = 0.05$ ), implying the success of the proposed method in the accurate and precise determination of DAC.

By comparing to previously reported potentiometric methods for the determination of DAC[14,15], this work offers improvement in performance characteristics of the optimized sensors in terms of, response time, dynamic linear range, and detection limit (Table 7).

**Table 4**

Logarithm the selectivity coefficient for the proposed electrodes using separate solution method and matched potential method.

Foreign species (B)	Log $K_{DAC,B}^{pot}$							
	Sensor I		Sensor I'		Sensor II		Sensor II'	
	SSM	MPM	SSM	MPM	SSM	MPM	SSM	MPM
Na <sup>+</sup>	-1.00	-4.07	-0.91	-3.98	-1.80	-4.38	-1.52	-3.92
K <sup>+</sup>	-0.57	-2.73	-1.72	-3.60	-2.37	-2.98	-2.38	-3.29
NH <sub>4</sub> <sup>+</sup>	-1.10	-4.16	-0.86	-3.85	-1.90	-4.92	-1.18	-3.94
Ca <sup>2+</sup>	-3.43	-4.79	-2.36	-3.66	-6.43	-4.95	-3.83	-3.63
Mg <sup>2+</sup>	-5.00	-4.57	-3.05	-3.93	-5.13	-4.91	-3.95	-3.55
Cu <sup>2+</sup>	-3.67	-2.71	-1.78	-2.68	-3.93	-4.16	-2.23	-3.86
Co <sup>2+</sup>	-4.53	-4.38	-2.82	-3.75	-5.40	-4.40	-3.09	-3.97
Mn <sup>2+</sup>	-3.93	-4.74	-2.30	-3.86	-4.43	-4.88	-2.98	-4.11
Fe <sup>3+</sup>	-1.46	-2.59	+1.19	+0.18	-1.40	-3.59	+1.06	+0.13
SOF	-	-1.63	-	-1.13	-	-1.49	-	-1.12
LED	-	-1.08	-	-1.30	-	-1.42	-	-1.45
Dopamine	-	-3.25	-	-3.01	-	-4.29	-	-2.91
Glycine	-	-4.07	-	-3.13	-	-4.37	-	-3.20
Alanine	-	-4.38	-	-3.97	-	-4.52	-	-3.97
Histidine	-	-4.17	-	-3.49	-	-4.42	-	-3.67
Lysine	-	-3.99	-	-3.57	-	-4.14	-	-3.51
Glucose	-	-4.29	-	-3.06	-	-5.09	-	-3.22
Soluble starch	-	-4.71	-	-3.97	-	-5.02	-	-3.59

**Table 5**

Determination of DAC in tablets, and spiked serum and urine using standard addition method.

Sample	Sensor II		
	Taken ( $\mu\text{mol/L}$ )	Recovery $\pm$ SD	RSD
Daclavicyr® (60 mg/tablet)	1	99.71 $\pm$ 0.89	0.90
	5	99.25 $\pm$ 0.65	0.66
	10	100.97 $\pm$ 1.37	1.35
Spiked serum	1	100.35 $\pm$ 0.79	0.79
	5	101.10 $\pm$ 1.19	1.18
	10	101.42 $\pm$ 0.76	0.75
Spiked urine	1	100.13 $\pm$ 1.26	1.26
	5	100.98 $\pm$ 1.54	1.53
	10	100.47 $\pm$ 1.30	1.30

SD: standard deviation, RSD: relative standard deviation, N = 4 replicates.

**Table 6**Statistical comparison between data obtained by sensors II, and HPLC reference method [29] for 5  $\mu\text{mol/L}$  Daclavicyr® tablet sample.

Method	Recovery <sup>a</sup> $\pm$ SD	F-calculated (9.28) <sup>b</sup>	t-calculated (2.45) <sup>c</sup>
HPLC [29]	100.23 $\pm$ 0.53	-	-
Sensor II	99.25 $\pm$ 0.65	1.51	2.32

<sup>a</sup>average of four determinations, <sup>b</sup> tabulated F-value at P = 0.05, <sup>c</sup> tabulated t-value at P = 0.05 and 6 degrees of freedom.

#### 4. Conclusion

In this work, Dibenzo-18-Crown-6-based carbon paste sensors were developed for the determination of DAC in its pure form, Daclavicyr® tablets, serum, and urine samples. The best analytical performance of two sensors referred to as sensor I and sensor II, which exhibited wide linear response range of  $5.0 \times 10^{-9}$  –  $1.0 \times 10^{-3}$  mol/L, with Nernstian slopes of  $29.8 \pm 1.18$  and  $29.5 \pm 1.00$  mV/decade, LOD of  $4.8 \times 10^{-9}$  and  $3.2 \times 10^{-9}$  mol/L, and instantaneous response times of 5–8 and 5–6 s, respectively, with great reversibility and no memory effect. The proposed sensors showed great selectivity towards DAC in presence of many metal cations, sugars, amino acids, dopamine, and other anti-HCV drugs (SOF and LED). In addition, the two sensors were applied for the determination of DAC in the above-mentioned samples, with high

**Table 7**

Comparison between performance characteristics of optimized sensors I and II in this work and the sensors developed in previously reported potentiometric methods[14,15].

Comparison	This work		Dear et.al. [14]	Eldin et. al. [15]
	CPE (Sensor I)	CPE (Sensor II)	SC-SPISE	PVC
Sensing element(s)	DB18C6 and Na-TPB	DB18C6 and Na-TImB	DAC-TPB and MWCNT	DAC-TPB
Slope, mV/decade	29.8	29.5	31.0	28.7
Linear range, M	$5 \times 10^{-9}$ – $10^{-3}$	$5 \times 10^{-9}$ – $10^{-3}$	$10^{-5}$ – $10^{-2}$	$10^{-6}$ – $10^{-3}$
LOD, nM	4.9	3.2	870	110
Response time, s	5–8	6–8	< 15	40

SC-SPISE – solid-contact screen printed ion-selective electrode, PVC – conventional polyvinyl chloride membrane electrode, DAC-TPB – daclavicyr-tetraphenylborate ion-exchanger, MWCNTs – multiwalled carbon nanotubes.

accuracy (recovery values ranging from 99.25 to 101.42%), and precision (relative standard deviation in the range of 0.79 to 1.53%). Finally, the proposed method was compared to a reference method (HPLC), and statistical analysis of data revealed compatible results of the methods.

#### Declaration of Competing Interest

The authors declare that they have no known competing financial interests or personal relationships that could have appeared to influence the work reported in this paper.

#### Acknowledgements

The authors would like to present their thanks to European Egyptian Pharmaceutical Industries (EETI), for kindly providing the DAC, SOF, and LED raw materials used in this work.

#### Appendix A. Supplementary data

Supplementary data to this article can be found online at <https://doi.org/10.1016/j.microc.2022.107276>.

## References

- [1] I. Waked, G. Esmat, A. Elsharkawy, M. El-Serafy, W. Abdel-Razek, R. Ghalab, G. Elshishiney, A. Salah, S. Abdel Megid, K. Kabil, M.H. El-Sayed, H. Dabbous, Y. El Shazly, M. Abo Sliman, K. Abou Hashem, S. Abdel Gawad, N. El Nahas, A. El Sobky, S. El Sonbaty, H. El Tabakh, E. Emad, H. Gemeah, A. Hashem, M. Hassany, N. Hefnawy, A.N. Hemida, A. Khadary, K. Labib, F. Mahmoud, S. Mamoun, T. Marei, S. Mekky, A. Meshref, A. Othman, O. Ragab, E. Ramadan, A. Rehan, T. Saad, R. Saeed, M. Sharshar, H. Shawky, M. Shawky, W. Shehata, H. Soror, M. Taha, M. Talha, A. Tealaab, M. Zein, A. Hashish, A. Cordie, Y. Omar, E. Kamal, I. Ammar, M. AbdAlIla, W. El Akel, W. Doss, H. Zaid, Screening and Treatment Program to Eliminate Hepatitis C in Egypt, *New Engand J. Med.* 382 (12) (2020) 1166–1174.
- [2] I. Elghitany, Hepatitis C Virus Infection in Egypt: Current Situation and Future Perspective, *Journal of High Institute of Public Health* 49 (1) (2019) 1–9.
- [3] A. Elgharably, A.I. Gomaa, M.M.E. Crossey, P.J. Norsworthy, I. Waked, S.D. Taylor-Robinson, Hepatitis C in Egypt – past, present, and future, *Int. J. Gen. Med.* 10 (2017) 1–6, <https://doi.org/10.2147/IJGM.S119301>.
- [4] A.M. Metwally, D.M. Elmosalami, H. Elhariri, L.A. El Etreby, A. Aboulghate, M. M. El-Sonbaty, A. Mohsen, R.M. Saleh, G.A. Abdel-Latif, S. Samy, S.E. El Deeb, A. M. Fathy, M.M. Salah, M.A. Abdel Mawla, H.M. Imam, N.A. Ibrahim, F.A. Shaaban, R.Y. Elamir, M. Abdelrahman, M.H. El-Sayed, Accelerating Hepatitis C virus elimination in Egypt by 2030: A national survey of communication for behavioral development as a modelling study, *PLoS One.* 16 (2021) 1–21, <https://doi.org/10.1371/journal.pone.0242257>.
- [5] M.A. Smith, R.E. Regal, R.A. Mohammad, Daclatasvir: A NS5A Replication Complex Inhibitor for Hepatitis C Infection, *Ann. Pharmacother.* 50 (2016) 39–46, <https://doi.org/10.1177/1060028015610342>.
- [6] M. Shabani, B. Sadegh Ehdai, F. Fathi, R. Dowran, A mini-review on sofosbuvir and daclatasvir treatment in coronavirus disease 2019, *New Microbes New Infect.* 42 (2021), 100895, <https://doi.org/10.1016/j.nmni.2021.100895>.
- [7] A.F.M.Z. Zein, C.S. Sulistiyana, W.M. Raffaello, A. Wibowo, R. Pranata, Sofosbuvir with daclatasvir and the outcomes of patients with COVID-19: A systematic review and meta-analysis with GRADE assessment, *Postgrad. Med. J.* (2021), <https://doi.org/10.1136/POSTGRADMEDJ-2021-140287>.
- [8] G. Esлами, S. Mousaviasl, E. Radmanesh, S. Jelvy, S. Bitaraf, B. Simmons, H. Wentzel, A. Hill, A. Sadeghi, J. Freeman, S. Salmanzadeh, H. Esmaeilian, M. Mobarak, R. Tabibi, A.H. Jafari Kashi, Z. Lotfi, S.M. Talebzadeh, A. Wickramatilake, M. Momtazan, M.H. Farsani, S. Marjani, S. Mobarak, The impact of sofosbuvir/daclatasvir or ribavirin in patients with severe COVID-19, *J. Antimicrob. Chemother.* 75 (2020) 3366–3372, <https://doi.org/10.1093/JAC/DKAA331>.
- [9] C.Q. Sacramento, N. Fintelman-Rodrigues, J.R. Temerozo, A. de P.D. Da Silva, S. da S.G. Dias, C. dos S. da Silva, A.C. Ferreira, M. Mattos, C.R.R. Pao, C.S. de Freitas, V. C. Soares, L.V.B. Hoelz, T.V.A. Fernandes, F.S.C. Branco, M.M. Bastos, N. Boechat, F.B. Saraiva, M.A. Ferreira, S. Jockusch, X. Wang, C. Tao, M. Chien, W. Xie, R.K.R. Rajoli, C.S.G. Pedrosa, G. Vitoria, L.R.Q. Souza, L. Goto-Silva, M.Z. Guimaraes, S.K. Rehen, A. Owen, F.A. Bozza, D.C. Bou-Habib, J. Ju, P.T. Bozza, T.M.L. Souza, In vitro antiviral activity of the anti-HCV drugs daclatasvir and sofosbuvir against SARS-CoV-2, the aetiological agent of COVID-19, *J. Antimicrob. Chemother.* 76 (2021) 1874–1885, <https://doi.org/10.1093/JAC/DKAB072>.
- [10] F.M. El-badawy, M.A. Mohamed, H.S. El-Desoky, Fabrication of an electrochemical sensor based on manganese oxide nanoparticles supported on reduced graphene oxide for determination of subnanomolar level of anti-hepatitis C daclatasvir in the formulation and biological models, *Microchem. J.* 157 (2020), <https://doi.org/10.1016/j.microc.2020.104914>.
- [11] A. Almahri, M.A. Abdel-Lateef, Applying different spectroscopic techniques for the selective determination of daclatasvir using merbromin as a probe: Applications on pharmaceutical analysis, *Luminescence.* (2021) 1–9, <https://doi.org/10.1002/bio.4099>.
- [12] S.S.H. Shah, M.I. Nasiri, H. Sarwar, A. Ali, S.B.S. Naqvi, S. Anwer, M. Kashif, RP-HPLC method development and validation for quantification of daclatasvir dihydrochloride and its application to pharmaceutical dosage form, *Pak. J. Pharm. Sci.* 34 (2021) 951–956, [10.36721/PJPS.2021.34.3.REG.951-956.1](https://doi.org/10.36721/PJPS.2021.34.3.REG.951-956.1).
- [13] O. Özbek, C. Berkel, Ö. Isildak, Applications of Potentiometric Sensors for the Determination of Drug Molecules in Biological Samples, *10.1080/10408347.2020.1825065.* (2020), [10.1080/10408347.2020.1825065](https://doi.org/10.1080/10408347.2020.1825065).
- [14] A.R. Derar, E.M. Hussien, Disposable Multiwall Carbon Nanotubes Based Screen Printed Electrochemical Sensor with Improved Sensitivity for the Assay of Daclatasvir: Hepatitis C Antiviral Drug, *IEEE Sens. J.* 19 (2019) 1626–1632, <https://doi.org/10.1109/JSEN.2018.2883656>.
- [15] A.S. Eldin, M.M. Abdel-Moety, A.S.M. El-Tantawy, A. Shalaby, M. El-Maamly, Simple potentiometric study for the detection of levofloxacin hydrochloride and daclatasvir dihydrochloride in pure form and pharmaceutical preparations, *Orient. J. Chem.* 34 (2018) 913–921, [10.13005/ojc/340240](https://doi.org/10.13005/ojc/340240).
- [16] I. Svancara, K. Kalcher, Chapter 11 – Carbon Paste Electrodes, in: R.C. Alkire, P. N. Bartlett, J. Lipkowski (Eds.), *Electrochem, Wiley-VCH Verlag GmbH & Co. KGaA, Carbon Electrodes, First edit.* 2015, pp. 379–423.
- [17] K.N. Mikhelson, M.A. Peshkova, Advances and trends in ionophore-based chemical sensors, *Russ. Chem. Rev.* 84 (6) (2015) 555–578.
- [18] R.P. Buck, E. Lindner, Recommendations for nomenclature of ion-selective electrodes (IUPAC recommendations, 1994), *Pure Appl. Chem.* 66 (1994) 2527–2536, <https://doi.org/10.1351/pac199466122527>.
- [19] N. Sakač, D. Madunić-čaćić, M. Karniš, B. Đurin, I. Kovač, M. Jozanović, The influence of plasticizers on the response characteristics of the surfactant sensor for cationic surfactant determination in disinfectants and antiseptics, *Sensors.* 21 (2021) 1–12, <https://doi.org/10.3390/s21103535>.
- [20] A.I. Vogel, *A Textbook of Quantitative Inorganic Analysis*, John Wiley, New York, 1966.
- [21] T. Mikysek, I. Švancara, K. Kalcher, M. Bartoš, K. Vytrás, J. Ludvík, New approaches to the characterization of carbon paste electrodes using the ohmic resistance effect and qualitative carbon paste indexes, *Anal. Chem.* 81 (15) (2009) 6327–6333, <https://doi.org/10.1021/ac9004937>.
- [22] V. Jagadabi, P.V. Nagendra Kumar, K. Mahesh, S. Pamidi, L.A. Ramaprasad, D. Nagaraju, A Stability-Indicating UPLC Method for the Determination of Potential Impurities and Its Mass by a New QDa Mass Detector in Daclatasvir Drug Used to Treat Hepatitis C Infection, *J. Chromatogr. Sci.* 57 (2019) 44–53, <https://doi.org/10.1093/chromsci/bmy079>.
- [23] Clinical Pharmacology and Biopharmaceutics Review(s), (n.d.), [https://www.accessdata.fda.gov/drugsatfda\\_docs/nda/2015/206843Orig1s000ClinPharmR.pdf](https://www.accessdata.fda.gov/drugsatfda_docs/nda/2015/206843Orig1s000ClinPharmR.pdf).
- [24] Y. Umezawa, P. Bühlmann, K. Umezawa, K. Tohda, S. Amemiya, Potentiometric selectivity coefficients of ion-selective electrodes Part I. Inorganic cations (Technical report), *Pure Appl. Chem.* 72 (2000) 1851–2082, <https://doi.org/10.1351/pac197437040439>.
- [25] V.P.Y. Gadzekpo, G.D. Christian, Determination of selectivity coefficients of ion-selective electrodes by a matched-potential method, *Anal. Chim. Acta.* 164 (1984) 279–282, [https://doi.org/10.1016/S0003-2670\(00\)85640-8](https://doi.org/10.1016/S0003-2670(00)85640-8).
- [26] M.R. Ganjali, N. Motakef-Kazami, F. Faridbod, S. Khoei, P. Norouzi, Determination of Pb<sup>2+</sup> ions by a modified carbon paste electrode based on multi-walled carbon nanotubes (MWCNTs) and nanosilica, *J. Hazard. Mater.* 173 (1–3) (2010) 415–419, <https://doi.org/10.1016/j.jhazmat.2009.08.101>.
- [27] F.M. Abdel-Haleem, M. Saad, A. Barhoum, M. Bechelany, M.S. Rizk, PVC membrane, coated-wire, and carbon-paste ion-selective electrodes for potentiometric determination of galantamine hydrobromide in physiological fluids, *Mater. Sci. Eng. C.* 89 (2018) 140–148, <https://doi.org/10.1016/j.msec.2018.04.001>.
- [28] S.T. Hassib, E.A. Taha, E.F. Elkady, G.H. Barakat, Reversed-Phase Liquid Chromatographic Method for Determination of Daclatasvir Dihydrochloride and Study of Its Degradation Behavior, *Chromatographia.* 80 (7) (2017) 1101–1107, <https://doi.org/10.1007/s10337-017-3321-3>.
- [29] S. Amemiya, P. Bühlmann, E. Pretsch, B. Rusterholz, Y. Umezawa, Cationic or anionic sites? Selectivity optimization of ion-selective electrodes based on charged ionophores, *Anal. Chem.* 72 (7) (2000) 1618–1631, <https://doi.org/10.1021/ac991167h>.
- [30] D. Ammann, E. Pretsch, W. Simon, E. Lindner, A. Bezegh, E. Pungor, Lipophilic salts as membrane additives and their influence on the properties of macro- and micro-electrodes based on neutral carriers, *Anal. Chim. Acta.* 171 (1985) 119–129, [https://doi.org/10.1016/S0003-2670\(00\)84189-6](https://doi.org/10.1016/S0003-2670(00)84189-6).
- [31] S. Wakida, T. Masadome, T. Imato, S. Kurosawa, Y. Shibutani, Response Mechanism of Additive Salt Effects of Potassium-Selective Neutral Carrier Based Electrode Using Their Liquid Membrane Based Ion-Sensitive Field-, *Anal. Sci.* 17 (Supplement) (2001) 15–18, [http://www.soc.nii.ac.jp/jsac/analsci/ICAS2001/pdfs/1600/1671\\_p4073n.pdf](http://www.soc.nii.ac.jp/jsac/analsci/ICAS2001/pdfs/1600/1671_p4073n.pdf).
- [32] E. Bakker, P. Bühlmann, E. Pretsch, Carrier-based ion-selective electrodes and bulk optodes. 1. General characteristics, *Chem. Rev.* 97 (8) (1997) 3083–3132, <https://doi.org/10.1021/cr940394a>.
- [33] A.A. Maryott, E.R. Smith, Table of Dielectric Constants of Pure Liquids, NBS Circul, National Bureau of Standards, Washington 25. D. C. 1951.
- [34] T. Rosatzin, E. Bakker, K. Suzuki, W. Simon, Lipophilic and immobilized anionic additives in solvent polymeric membranes of cation-selective chemical sensors, *Anal. Chim. Acta.* 280 (2) (1993) 197–208, [https://doi.org/10.1016/0003-2670\(93\)85122-Z](https://doi.org/10.1016/0003-2670(93)85122-Z).
- [35] T. Alaviuhkola, J. Bobacka, M. Nissinen, K. Rissanen, A. Ivaska, J. Pursiainen, Synthesis, characterization, and complexation of tetraarylborates with aromatic cations and their use in chemical sensors, *Chem. – A Eur. J.* 11 (7) (2005) 2071–2080, <https://doi.org/10.1002/chem.200400992>.
- [36] Daclatasvir dihydrochloride | DrugBank Online, (n.d.), <https://go.drugbank.com/salts/DBSALT01166> (accessed June 28, 2021).
- [37] J. Mohanty, S.D. Choudhury, N. Barooah, H. Pal, A.C. Bhasikuttan, Mechanistic Aspects of Host-Guest Binding in Cucurbiturils: Physicochemical Properties, Second Edi, Elsevier (2017), <https://doi.org/10.1016/b978-0-12-409547-2.11028-5>.
- [38] S. Krait, A. Salgado, C. Villani, L. Naumann, C. Neusüß, B. Chankvetadze, G.K. E. Scriba, Unusual complexation behavior between daclatasvir and  $\gamma$ -Cyclodextrin. A multiplatform study, *J. Chromatogr. A.* (1628 (2020)), 461448, <https://doi.org/10.1016/j.chroma.2020.461448>.
- [39] S. Krait, A. Salgado, P. Peluso, M. Malanga, T. Sohajda, G. Benkovic, L. Naumann, C. Neusüß, B. Chankvetadze, G.K.E. Scriba, Complexation of daclatasvir by single isomer methylated  $\beta$ -cyclodextrins studied by capillary electrophoresis, NMR spectroscopy and mass spectrometry, *Carbohydr. Polym.* (2021), 118486, <https://doi.org/10.1016/j.carbpol.2021.118486>.
- [40] C.J. Pedersen, Cyclic Polyethers and Their Complexes with Metal Salts, *J. Am. Chem. Soc.* 89 (26) (1967) 7017–7036, <https://doi.org/10.1021/ja01002a035>.
- [41] S.M. Mostafa, A.A. Farghali, M.M. Khalil, Novel potentiometric sensors based on  $\beta$ -cyclodextrin and dibenzo 18-crown-6 ionophores/mesoporous silica nanoparticles for clidinium determination, *Int. J. Electrochem. Sci.* 15 (2020) 3347–3364, [10.20964/2020.04.48](https://doi.org/10.20964/2020.04.48).
- [42] C.M. Choi, J. Heo, N.J. Kim, Binding selectivity of dibenzo-18-crown-6 for alkali metal cations in aqueous solution: A density functional theory study using a continuum solvation model, *Chem. Cent. J.* 6 (2012) 1–8.

- [44] A. Kumar, S.K. Mittal, PVC based dibenzo-18-crown-6 electrode for Ca (II) ions 99 (2004) 340–343, <https://doi.org/10.1016/j.snb.2003.11.033>.
- [45] S. V. Smirnova, I.I. Torocheshnikova, A.A. Formanovsky, I. V. Pletnev, Solvent extraction of amino acids into a room temperature ionic liquid with dicyclohexano-18-crown-6, (2004) 1369–1375. 10.1007/s00216-003-2398-8.
- [46] P. Ottiger, C. Pfaffen, R. Leist, S. Leutwyler, R.A. Bachorz, W. Klopper, Strong N-H... $\pi$  hydrogen bonding in amide-benzene interactions, *J. Phys. Chem. B* 113 (2009) 2937–2943, <https://doi.org/10.1021/JP8110474>.
- [47] A.K. Lemmens, P. Chopra, D. Garg, A.L. Steber, M. Schnell, W.J. Buma, A.M. Rijs, High-resolution infrared spectroscopy of naphthalene and acenaphthene dimers, 10.1080/00268976.2020.1811908. 119 (2020). 10.1080/00268976.2020.1811908.
- [48] U. Erlekam, M. Frankowski, G. Meijer, G. Von Helden, An experimental value for the Blu C-H stretch mode in benzene, *J. Chem. Phys.* 124 (2006) 171101–171104, <https://doi.org/10.1063/1.2198828>.
- [49] G. Platzer, M. Mayer, A. Beier, S. Brüschiweiler, J.E. Fuchs, H. Engelhardt, L. Geist, G. Bader, J. Schörghuber, R. Lichtenecker, B. Wolkerstorfer, D. Kessler, D. B. McConnell, R. Konrat, PI by NMR: Probing CH- $\pi$  Interactions in Protein-Ligand Complexes by NMR Spectroscopy, *Angew. Chemie* 132 (2020) 14971–14978, <https://doi.org/10.1002/ange.202003732>.
- [50] M.N.C. Zarycz, C. Fonseca Guerra, NMR <sup>1</sup>H-Shielding Constants of Hydrogen-Bond Donor Reflect Manifestation of the Pauli Principle, *J. Phys. Chem. Lett.* 9 (13) (2018) 3720–3724.
- [51] D. Grieshaber, R. MacKenzie, J. Vörös, E. Reimhult, Electrochemical Biosensors – Sensor Principles and Architectures, *Sensors (Basel)* 8 (2008) 1400, <https://doi.org/10.3390/S80314000>.
- [52] F.M. Abdel-Haleem, S. Mahmoud, N.E.T. Abdel-Ghani, R.M. El Nashar, M. Bechelany, A. Barhoum, Polyvinyl chloride modified carbon paste electrodes for sensitive determination of levofloxacin drug in serum, urine, and pharmaceutical formulations, *Sensors* 21 (2021) 1–23, <https://doi.org/10.3390/S21093150>.
- [53] E. Bakker, Determination of Unbiased Selectivity Coefficients of Neutral Carrier-Based Cation-Selective Electrodes, *Anal. Chem.* 69 (6) (1997) 1061–1069, <https://doi.org/10.1021/ac960891m>.
- [54] R. Eugster, P.M. Gehrig, W.E. Morf, U.E. Spichiger, W. Simon, Selectivity-Modifying influence of Anionic Sites in Neutral-Carrier-Based Membrane Electrodes, *Anal. Chem.* 63 (20) (1991) 2285–2289, <https://doi.org/10.1021/ac00020a017>.
- [55] C. Wardak, A Comparative Study of Cadmium Ion-Selective Electrodes with Solid and Liquid Inner Contact, *Electroanalysis* 24 (1) (2012) 85–90, <https://doi.org/10.1002/elan.201100362>.
- [56] J.D.R. Thomas, G.J. Moody, T.H. Ryan, B. Fleet, M. Whitfield, K. Garbett, A. Craggs, Ion-selective electrodes, *Proc. Anal. Div. Chem. Soc.* 12 (1975) 48–64, <https://doi.org/10.1039/AD9751200048>.
- [57] E. Bakker, K. Chumbimuni-Torres, Modern directions for potentiometric sensors, *J. Braz. Chem. Soc.* 19 (2008) 621–629, <https://doi.org/10.1590/S0103-50532008000400003>.
- [58] M. Fibbioli, W.E. Morf, M. Badertscher, N.F. de Rooij, E. Pretsch, Potential drifts of solid-contacted ion-selective electrodes due to zero-current ion fluxes through the sensor membrane, *Electroanalysis* 12 (16) (2000) 1286–1292.
- [59] I. Švancara, K. Kalcher, A. Walcarius, K. Vytras, *Electroanalysis with carbon paste electrodes*, (2012).
- [60] E. Bakker, E. Pretsch, P. Bühlmann, Selectivity of potentiometric ion sensors, *Anal. Chem.* 72 (6) (2000) 1127–1133, <https://doi.org/10.1021/ac991146n>.
- [61] S. Ogawara, J.L. Carey, X.U. Zou, P. Bühlmann, Donnan Failure of Ion-Selective Electrodes with Hydrophilic High-Capacity Ion-Exchanger Membranes, *ACS Sensors* 1 (1) (2016) 95–101.
- [62] Fatehy abdel-haleem M., Carbon-based Nanosensors for Salicylate Determination in Pharmaceutical Preparations, *electroanalysis* 31 (4) (2019) 778, <https://doi.org/10.1002/elan.201800728>.
- [63] Fatehy abdel-haleem M., Polyvinyl chloride modified carbon paste electrodes for sensitive determination of levofloxacin drug in serum, urine, and pharmaceutical formulations, *sensors* (2021).
- [64] fatehy abdel-haleem M., t-Butyl calixarene/Fe<sub>2</sub>O<sub>3</sub>@ MWCNTs composite-based potentiometric sensor for determination of ivabradine hydrochloride in pharmaceutical formulations, *Materials Science and Engineering: C* (2020).
- [65] abdel-haleem, Development of new potentiometric sensors for the determination of Proguanil hydrochloride in serum and urine, *chinese chemical letters* (2016).
- [66] fatehy abdel-haleem M., Highly selective thiourea-based bulk optode for determination of salicylate in spiked urine samples, *Aspirin® and Aspidocid®*, *Sensors and Actuators B: Chemical* (2016).
- [67] fatehy abdel-haleem M., et al., Molecularly imprinted polymer-based bulk optode for the determination of itopride hydrochloride in physiological fluids, *Biosensors and Bioelectronics* (2016).

**Yomna M. Ahmed** is an assistant lecturer at the department of chemistry at the faculty of science, Cairo University, Egypt, from where she received her M.Sc. degree in 2019. She is currently pursuing her Ph.D. degree in analytical chemistry. Her current research interest comprises the development of electrochemical sensors, ionophore-based sensors, miniaturized sensors, sensors of framework-based materials, molecularly imprinted materials, nanostructured materials, and carbon-based materials.

**Sayed S. Badawy** is full professor at department of chemistry at faculty of science, Cairo university, Egypt. He is the coauthor of more than 70 research publications. His current interest comprises the use of simple and mixed ionophores for the development of electrochemical sensors for liquid samples, ion-selective electrodes, solid-contact ion-selective electrodes, potentiometric sensors, ionophore-based sensors, conducting polymer-based sensors, nanostructured materials, and carbon-based materials for the pharmaceutical determinations' application.

**Fatehy M. Abdel-Haleem** is an associate professor of Analytical Chemistry, Chemistry Department, Faculty of Science, Cairo University, Cairo, Egypt. He is the technical manager of chemistry lab in the center of hazards mitigation, environmental studies and research (CHMESR) in Cairo university. He received his MSc. & Ph.D. in Analytical Chemistry from Cairo University. He is the coauthor of more than 20 research publications. His scientific interests focus on carbon and metal nanomaterials for electrochemical and optical sensors. His research concerns using different modifiers such as multi-walled carbon nanotubes, graphene, graphene oxide and reduced graphene oxide to enhance the sensor performance.